ISSN: 2688-8645

Investigation of Multi-Cycle Absorption Performance of Organic Amines under Low-Flux and Low-Partial-Pressure CO_2 Conditions

Yuan Tao, Bingru Zhang

College of Environmental Science and Engineering, Tongji University, Shanghai, 200092, China

Abstract

To evaluate the stability of amine absorbents in low-flow, low-concentration, and low-partial-pressure CO_2 absorption-desorption cycles, two key performance parameters were analyzed: the ratio of apparent cycle capacity to maximum cycle capacity (ACCR/MCCR) and the 20-cycle retention capacity. These metrics were applied to assess the absorption stability, desorption properties, and cyclical performance of ethanolamine (MEA), triethylenetetramine (TETA), N-methyldiethanolamine (MDEA), and the MDEA/TETA blend. Experimental results demonstrated that the ACCR/MCCR directly quantifies the divergence between CO_2 absorption efficiency under constrained operational conditions and the theoretical maximum capacity, while the 20-cycle retention capacity reflects the evolution of CO_2 transport capability during repeated cycles. The MDEA/TETA mixed absorbent achieved the highest ACCR/MCCR of 78.10%, indicating minimal efficiency loss under suboptimal conditions. Additionally, it maintained a stable 20-cycle capacity of 0.75 mol CO_2/mol amine, showcasing robust cyclical durability. This combination of high ACCR/MCCR and sustained capacity highlights the MDEA/TETA system's potential for industrial applications, particularly in capturing CO_2 from flue gas generated by fossil fuel combustion, where stability under fluctuating low-concentration conditions is critical.

Keywords

CCUS; Post-combustion Capture; Amine Absorbent; Cycle Capacity; Cyclic Absorption Stability.

1. Introduction

To evaluate the stability of amine absorbents in low-flow, low-concentration, and low-partial-pressure CO_2 absorption-desorption cycles, two key performance parameters were analyzed: the ratio of apparent cycle capacity to maximum cycle capacity (ACCR/MCCR) and the 20-cycle retention capacity. These metrics were applied to assess the absorption stability, desorption properties, and cyclical performance of ethanolamine (MEA), triethylenetetramine (TETA), N-methyldiethanolamine (MDEA), and the MDEA/TETA blend. Experimental results demonstrated that the ACCR/MCCR directly quantifies the divergence between CO_2 absorption efficiency under constrained operational conditions and the theoretical maximum capacity, while the 20-cycle retention capacity reflects the evolution of CO_2 transport capability during repeated cycles. The MDEA/TETA mixed absorbent achieved the highest ACCR/MCCR of 78.10%, indicating minimal efficiency loss under suboptimal conditions. Additionally, it maintained a stable 20-cycle capacity of 0.75 mol CO_2/mol amine, showcasing robust cyclical durability. This combination of high ACCR/MCCR and sustained capacity highlights the MDEA/TETA system's potential for industrial applications, particularly in capturing CO_2 from flue gas generated by fossil fuel combustion, where stability under fluctuating low-concentration conditions is critical. Since the onset of industrialization in 1850, the escalating use of fossil fuels has driven a continuous rise in CO_2 emissions, resulting in a global temperature increase of approximately 1.1°C compared to pre-industrial levels, with temperatures still climbing [1]. Global warming has profoundly impacted natural systems, exacerbating droughts, floods, extreme weather events, sea-level rise, and biodiversity loss, posing unprecedented risks to human habitats [2]. In 2023, global energy-related CO_2 emissions reached a record high of 37.4 billion tons, with approximately two-thirds originating from fossil fuel combustion [3]. CO_2 emitted from fossil fuel combustion is characterized by low partial pressure and low concentration [4, 5], making chemical solvent absorption methods particularly suitable for its capture under these conditions [6, 7]. Among chemical absorption techniques, organic amine solutions are widely studied due to their rapid CO_2 absorption rates and reusability, outperforming hot potassium carbonate and ammonia-based methods [8-10]. However, conventional primary and secondary amine absorbents exhibit low absorption-desorption cycle capacities. For example, monoethanolamine (MEA) achieves only 70% of its initial absorption capacity after regeneration at 40°C (absorption) and 130°C (desorption) [11]. Tertiary amines like methyldiethanolamine (MDEA) demonstrate full desorption efficiency but suffer from slow absorption kinetics, with CO_2 loading capacities as low as 32% of MEA's performance under comparable condition [12, 13], leading to poor cyclic capacity. Although blended amines combining tertiary and polyamines show improved absorption performance, the stability of their cycle capacities over multiple cycles remains understudied. For instance, Song et al. [14]reported that a blend of MDEA and tetraethylenepentamine (TEPA) achieved an absorption capacity of 0.753 mol CO_2/mol amine at 40°C, with a cyclic capacity of 0.241–0.330 mol CO_2/mol amine (three times higher than MEA) under 40°C absorption and 293.15 K desorption. Hafizi et al. [15] found that the MDEA-TEPA blend exhibited enhanced regeneration rates compared to pure MEA but slower rates than pure MDEA. However, these findings primarily explain the initial absorption-desorption performance of the absorbents, leaving long-term stability unaddressed.

The stability of cyclic CO_2 absorption-desorption performance in organic amine absorbents over multiple cycles remains understudied. Hu Yanlong et al. [16] investigated the cycle capacity of phase-change absorbents (MEA and MDEA) over 10 absorption-desorption cycles, but their experiments employed high-concentration, high-partial-pressure CO_2 conditions, with a CO_2 flow rate of 250 mL/min per 20 g of absorbent. These findings are not applicable to low-flow, low-partial-pressure flue gas emissions, which typify real-world industrial applications of organic amine-based CO_2 capture. In practical engineering scenarios, flue gas CO_2 exhibits low flow rates, low concentrations, low partial pressures, and short absorption-desorption cycle durations [17]. Under such conditions, absorbents struggle to achieve saturation absorption or maximal desorption, necessitating more pragmatic parameters to evaluate their cyclic performance under constrained operational limits. Furthermore, few studies have systematically analyzed the evolution of cycle stability during repeated absorption-desorption processes.

During multiple absorption-desorption cycles, the cyclic absorption performance of absorbents inevitably degrades due to oxidative degradation, thermal decomposition, and other factors. To evaluate the cyclic absorption performance of organic amine absorbents under low-flow, low-concentration, and low-partial-pressure CO_2 conditions over repeated cycles, this study investigates two metrics: (1) Apparent cycle capacity as a percentage of maximum cycle capacity (ACCR/MCCR), quantifying the retained efficiency under constrained operational limits; (2) Stability of cycle capacity across 20 absorption-desorption cycles, assessing long-term performance degradation. Experiments simulated CO_2 conditions typical of post-combustion flue gas from fossil fuels—characterized by low flow rates, low concentrations, and low partial pressure. The absorption-desorption properties of MEA, MDE, TETA, and an MDEA/TETA blended amine were systematically studied. ACCR/MCCR and 20-cycle capacity were measured and compared to evaluate changes in cyclic absorption performance and stability across repeated cycles.

2. Organization of the Text

2.1. Materials

Commercial-grade CO_2 (99.999% purity) and N_2 (99.9% purity) were utilized. Ethanolamine (MEA, 99%, analytical grade), N-methyldiethanolamine (MDEA, 99%, analytical grade), triethylenetetramine (TETA, 99%, analytical grade), and hydrochloric acid (36–38%) were obtained from Sinopharm Chemical Reagent Co., Ltd. Aqueous solutions were prepared with the following compositions: 30 wt% MEA, 30 wt% TETA, 30 wt% MDEA, and a blended amine solution containing 20 wt% MDEA and 10 wt% TETA. A standardized sulfuric acid titrant solution with a concentration of $c(1/2H_2SO_4) = 1.0$ mol/L was prepared and calibrated for subsequent experimental procedures.

2.2. Methods

2.2.1. Absorption Experiment

The absorption experiments were conducted using the apparatus illustrated in Fig. 1(a). A 250 g aliquot of a 30% aqueous organic amine solution was added to a four-necked flask equipped with a reflux condenser, thermometer, stirrer, and sampling port. The solution was heated to a constant temperature of 40°C. A gas mixture of CO_2 and N_2 was prepared by adjusting the CO_2 volume fraction to 15%, total gas flow rate to 1000 mL/min, and total pressure to 1 atm using gas flow meters. The gas mixture was homogenized through a gas mixing and saturation unit before being introduced into the four-necked flask for CO_2 absorption. Samples were collected at regular intervals to measure the CO_2 loading of the absorbent solution. The absorption process was terminated when the CO_2 loading stabilized, yielding CO_2-rich liquid.

For titration, 1 mL of the sample was transferred to the titration setup shown in Fig. 1(c). An excess volume of acid (V_a, mL) was added to fully release CO_2 from the sample. The CO_2 content ($n_{CO_2,s}$, mol CO_2/mL) was calculated based on the volume difference (ΔV, mL) measured by the gas burette before and after the reaction, as expressed in Equation (1):

$$n_{CO_2,s} = \frac{\Delta V - V_a}{\frac{T}{273} \times 22.4} \tag{1}$$

where $n_{CO_2,s}$ represents the molar amount of CO_2 released from the sample, mol CO_2; ΔV is the difference in gas burette readings before and after sulfuric acid addition, mL; V_a is the volume of acid added, mL; T denotes the ambient temperature of the gas measurement apparatus during testing, K.

The CO_2 loading of the organic amine is calculated by dividing $n_{CO_2,s}$ by the molar amount of amine per mL of solution ($n_{amine,s}$, mol amine/mL), as expressed in Eq. (2) and Eq. (3):

$$\alpha = \frac{n_{CO_2,s}}{n_{amine,s}} \tag{2}$$

$$n_{amine,s} = \frac{n_{amine,t}}{V_{solution}} = \frac{\frac{W_{amine}}{M_{amine}}}{\frac{W_{solution}}{\rho_{solution}}} \tag{3}$$

where $n_{amine,t}$ is the molar amount of amine used to prepare the solution, mol; $V_{solution}$ is the volume of the prepared amine solution, mL; W_{amine} is the mass of the amine, g; M_{amine} is the molar mass of the amine, g/mol; $W_{solution}$ is the total mass of the solution, g; $\rho_{solution}$ is the solution density, g/mL.

To confirm that water retention and experimental apparatus maintained constant amine concentrations before and after absorption, the amine solutions were titrated with standardized H_2SO_4 using methyl orange as an indicator. A concentration difference of less than 2% between pre- and post-absorption samples [18] validated the assumption of stable amine concentration during CO_2 absorption.

2.2.2. Desorption Experiment

Desorption experiments were conducted using the apparatus shown in Fig. 1(b). After heating the oil bath to the target desorption temperature, CO_2-rich liquid was introduced into the desorption vessel, and timing commenced. Samples were collected periodically to measure residual CO_2 loading until stabilization, marking the end of desorption. The desorption efficiency, defined as the percentage of CO_2 released relative to the initial CO_2 loading in the rich solution, is given by Equation (4):

$$\eta_{de} = \frac{\alpha_r - \alpha_l}{\alpha_r} \times 100\% \tag{4}$$

Where η_{de} represents the desorption efficiency; α_r is the CO_2 loading of the rich solution before desorption, mol CO_2/mol amine; α_l is the CO_2 loading of the lean solution after desorption, mol CO_2/mol amine.

2.2.3. Absorption-desorption Cycle Experiment

A 250 g aqueous solution containing 30 wt% organic amine absorbent was charged into the absorption apparatus. Under controlled conditions (40°C, 0.1 MPa pressure), a gas mixture comprising 15 vol% CO_2 balanced with N_2 was introduced at a flow rate of 1000 mL/min. After 150 minutes of absorption, the CO_2-rich solution was obtained. This rich solution was subsequently subjected to desorption in an oil bath maintained at 125°C for 90 minutes, yielding the regenerated CO_2-lean solution. The lean solution was then recycled for the next absorption-desorption cycle. This process was repeated for 20 consecutive cycles, with the CO_2 loading of both rich and lean solutions measured after each cycle.

The cyclic capacity was defined as the difference in CO_2 loading between the CO_2-rich solution (after absorption) and the CO_2-lean solution (after desorption) within a single absorption-desorption cycle, which is calculated in Eq. (5):

$$CC = \alpha_r - \alpha_l \tag{5}$$

where, CC is the cyclic capacity, mol CO_2/mol amine.

The cyclic capacity obtained through absorption-desorption cycles conducted under predetermined time constraints is defined as the apparent cyclic capacity.

The maximum cyclic capacity of an absorbent is determined as the difference between the CO_2-rich solution loading at saturation absorption and the CO_2-lean solution loading achieved under maximum desorption efficiency, which is calculated in Eq. (6):

$$CC_{max} = \alpha_{rmax} - \alpha_{lmin} \tag{6}$$

where, CC_{max} is the maximum cyclic capacity, mol CO_2/mol amine; α_{rmax} is the CO_2 loading of the CO_2-rich solution which is in equilibrium, mol CO_2/mol amine; α_{lmin} is the CO_2 loading of the CO_2-lean solution which achieves the maximum desorption degree, mol CO_2/mol amine.

The attenuation rate of absorbent cyclic capacity was calculated by dividing the difference between the maximum cyclic capacity observed during 20 cycles and the capacity at the 20th cycle by the cycle interval between the occurrence of maximum capacity and the final (20th) cycle, which is calculated in Eq. (7):

$$\eta = \frac{CC_{high} - CC_{20}}{20 - C_{high}} \tag{7}$$

where CC_{high} is the maximum cyclic capacity observed across 20 cycles, mol CO_2/mol amine; CC_{20} is the cyclic capacity at the 20th cycle, mol CO_2/mol amine; C_{high} is the cycle number at which the maximum capacity was achieved.

It should be noted that CC_{high} corresponds to the highest cyclic capacity attainable by the absorbent under the cumulative effects of thermal decomposition and oxidative degradation over multiple cycles, which differs from CC_{max} in Equation (6) – the latter represents the theoretical maximum cyclic capacity for a single absorption-desorption cycle under idealized conditions.

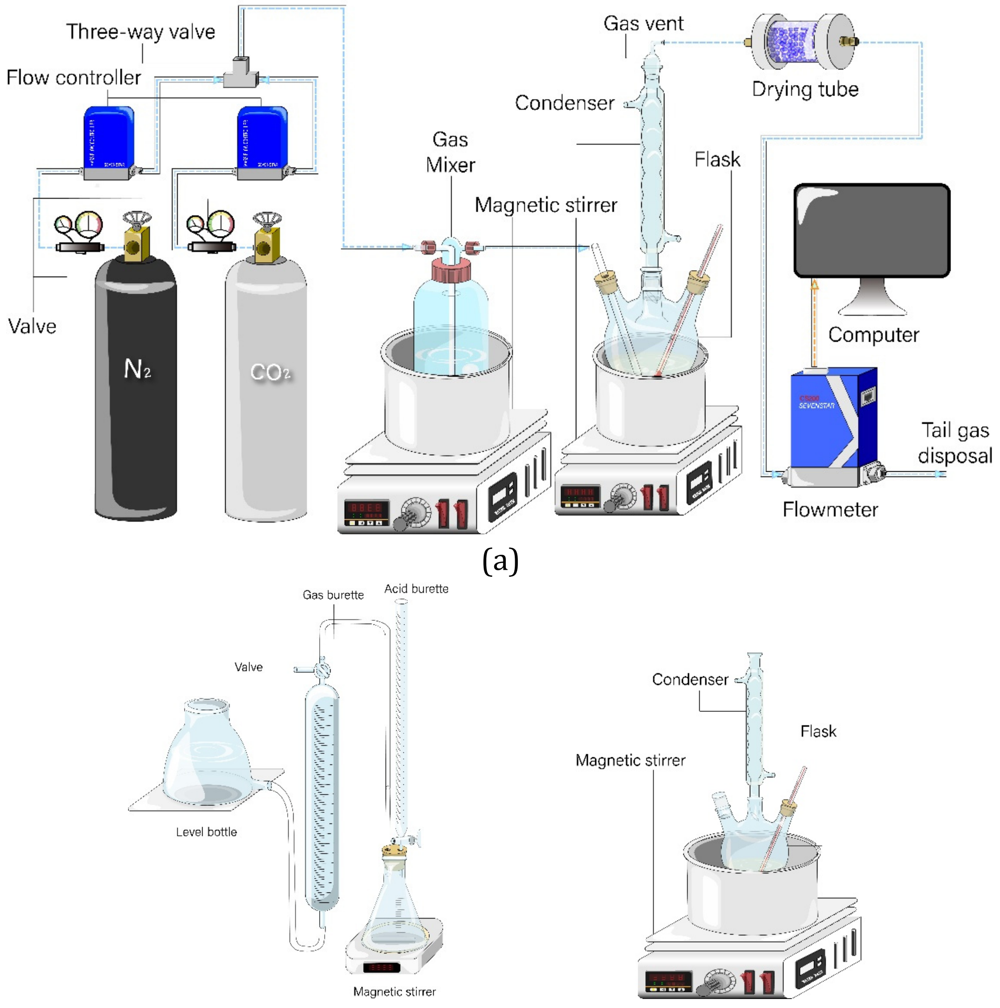

(a)

(b) (c)

Fig 1. Experimental apparatus ((a) absorption apparatus, (b) desorption apparatus, (c) titrimetric apparatus)

3. Results and Discutions

3.1. Absorption Performance

To verify the reliability of the absorption apparatus, the equilibrium solubility data of 30% MEA and 30% MDEA solutions obtained in this experiment were compared with literature values [19-21], as shown in Fig. 2. The experimental results confirm the reliability of the apparatus. The amine concentration variation was 0.17% for 30% MEA and 0.11% for 30% TETA, indicating that the amine solution concentration error before and after absorption remained below 2%. This confirms that the solution concentration can be considered constant during CO_2 absorption.

The CO_2 loading variations of four absorbents over time are illustrated in Fig. 3. The maximum CO_2 absorption capacities were determined as follows: 0.56 mol CO_2/mol amine for 30% MEA, 0.43 mol CO_2/mol amine for 30% MDEA, 1.69 mol CO_2/mol amine for 30% TETA, and 0.84 mol

CO_2/mol amine for the 20% MDEA + 10% TETA blend. These results demonstrate that absorption capacity increases with the number of amino groups per mole of amine molecule. Comparing MEA and MDEA, both containing one amino group per molecule, MEA exhibits higher maximum loading and faster saturation kinetics. This difference arises because MEA's primary amine group reacts directly with CO_2 to form primary carbamate which is shown in Eq. 8:

$$2RNH_2 + CO_2 \leftrightharpoons RNHCOO^- + RNH_3{}^+ \tag{8}$$

a nearly irreversible reaction at lower temperatures that enables full amino group participation given sufficient absorption time.

In contrast, MDEA's tertiary amine group cannot react directly with CO_2. Instead, it enhances solution alkalinity through protonation, catalyzing CO_2 conversion to bicarbonate Eq. 9 and Eq. 10:

$$R_1R_2R_3N + H_2O \leftrightharpoons R_1R_2R_3NH^+ + OH^- \tag{9}$$

$$CO_2 + OH^- \leftrightharpoons HCO_3{}^- \tag{10}$$

This process exhibits slower kinetics, and the declining alkalinity at higher CO_2 loadings inhibits further absorption under constant CO_2 partial pressure. Notably, the MDEA+TETA blend demonstrates superior performance compared to pure MDEA, achieving higher CO_2 loading (0.84 mol/mol) with a shorter saturation time (300 min) - half that of pure MDEA. This synergy between polyamine (TETA) and tertiary amine (MDEA) enhances both absorption capacity and kinetics, effectively addressing the inherent rate limitations of tertiary amines.

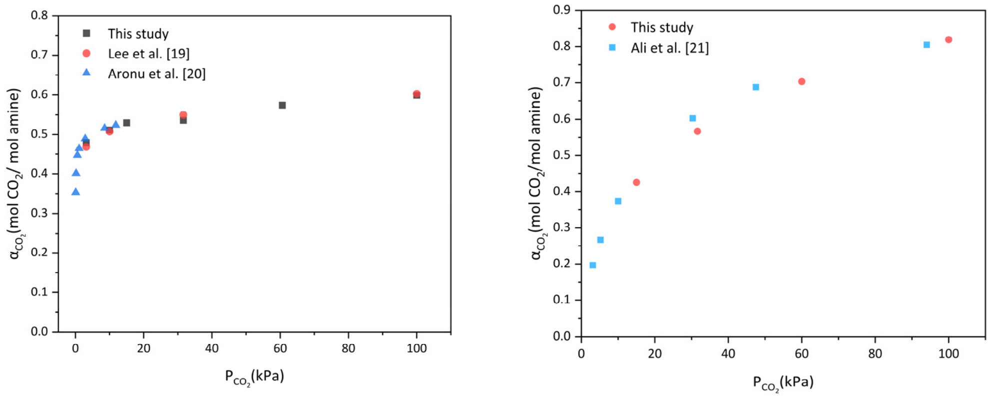

(a) (b)

Fig 2. The experimental values of equilibrium solubility under different partial pressure of CO_2 compared with those in literature (a. 30% MEA aqueous solution; b. 30% MDEA aqueous solution)

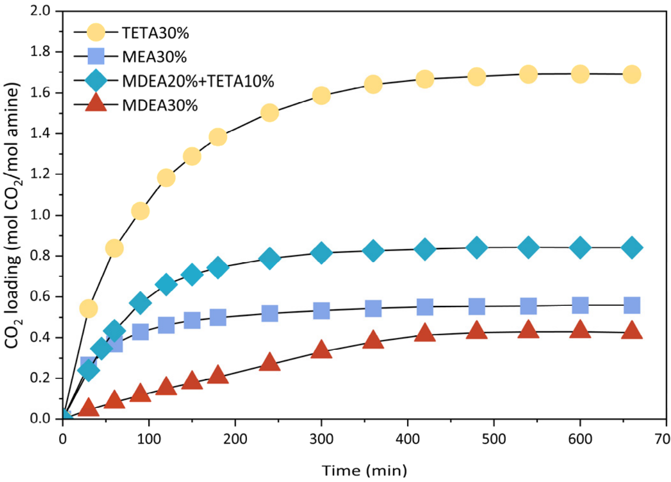

Fig 3. Change of CO_2 loading with time for four absorbents

3.2. Desorption Performance

Fig. 4 illustrates the temporal variation of CO_2 loading in MEA-rich solution under different desorption temperatures. The results demonstrate that at 125°C, MEA achieved a desorption rate of 70% after 90 minutes, reaching maximum desorption efficiency of 75% at 180 minutes. Lower desorption rates were observed at temperatures below 125°C for equivalent 90-minute durations. Notably, while the 130°C condition achieved 83% desorption in 90 minutes (88% maximum), electrical power measurements revealed its total energy consumption (3861.15 KJ) was 1.5 times higher than that of 125°C operation for equivalent duration, yielding merely 13% improvement in desorption efficiency. This marginal enhancement through elevated energy input proves economically unfavorable. More critically, higher desorption temperatures exacerbate oxidative and thermal degradation of organic amines [22]. Therefore, 125°C was selected as the optimal desorption temperature in this study.

The CO_2 loading and desorption efficiency of four absorbents during 125°C desorption (following 150-minute absorption at 125°C) are presented in Fig. 5. The maximum desorption efficiencies followed this descending order: MDEA > MDEA+TETA blend > TETA > MEA. MEA exhibited the lowest desorption performance with 66.89% efficiency after 90 minutes, attributable to the stable structure and high absorption enthalpy of primary carbamates formed through CO_2 reaction with its primary amine groups [23]. TETA demonstrated superior desorption (72.44% at 90 minutes) due to two synergistic mechanisms: 1) polycarbamates formed through multi-amine group participation exhibit lower absorption enthalpy than monofunctional carbamates, and 2) secondary carbamates derived from TETA's secondary amines possess inherently lower absorption enthalpy than primary carbamates [24]. As carbamate decomposition represents the reverse process of absorption (Equation 7), reduced absorption enthalpy directly translates to lower desorption energy requirements, explaining TETA's enhanced desorption efficiency compared to MEA.

Remarkably, MDEA achieved complete (100%) desorption as it forms bicarbonate species rather than carbamates during CO_2 absorption. These bicarbonate compounds exhibit lower stability and absorption enthalpy, enabling complete decomposition under thermal desorption conditions. The MDEA+TETA blended solution demonstrated 90.49% desorption efficiency at 90 minutes - 18.06% higher than pure TETA solution and approaching MDEA's full desorption capacity. This enhancement stems from MDEA's tertiary amine groups catalyzing the conversion of TETA-derived carbamates (from primary/secondary amines) into bicarbonate species. This synergistic interaction reduces the blended system's effective absorption enthalpy compared to pure TETA solution, thereby significantly improving desorption performance while maintaining favorable absorption characteristics.

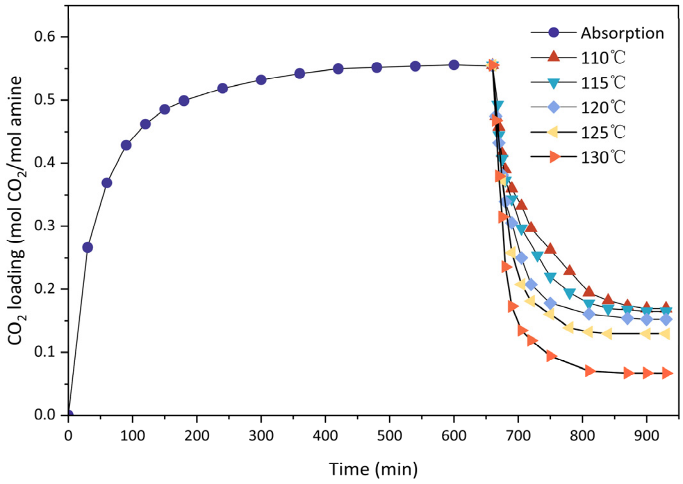

Fig 4. The change of CO_2 loading of MEA solution desorbed at 110 °C, 115 °C, 120 °C, 125 °C, 130 °C for 90 min

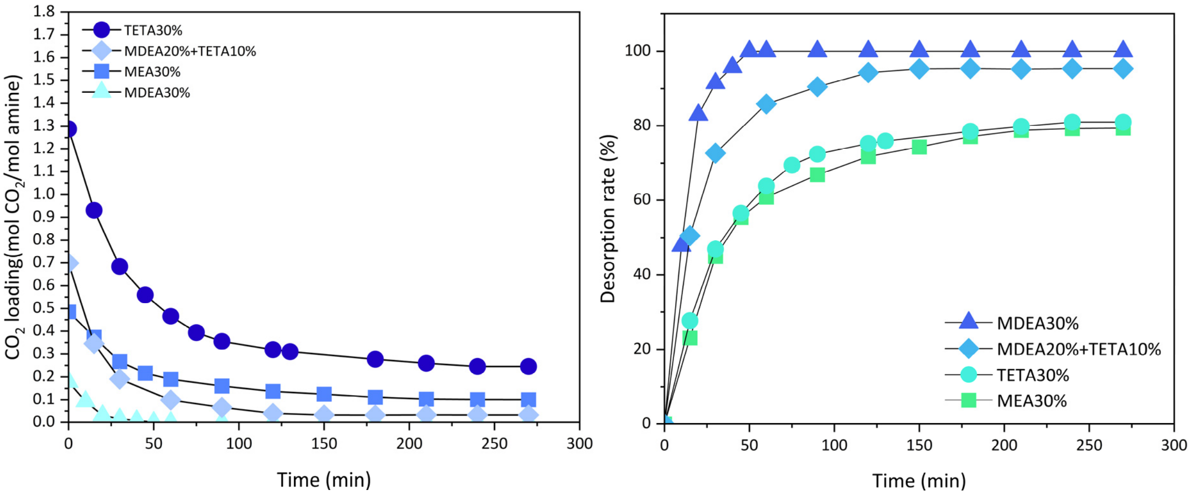

(a) (b)

Fig 5. (a) The change of CO_2 loading with time of four absorbents desorbed at 125 ℃; (b) The change of desorption rate with time of four absorbents desorbed at 125 ℃

3.3. Cyclic Stability

3.3.1. ACCR/MCCR Analysis

Under absorption-desorption cyclic experimental conditions, the maximum cyclic capacities of four absorbents were determined as follows: 0.45 mol CO_2/mol amine for MEA, 1.41 mol CO_2/mol amine for TETA, 0.43 mol CO_2/mol amine for MDEA, and 0.81 mol CO_2/mol amine for the MDEA+TETA blend, as illustrated in Fig. 6. The apparent cyclic capacities measured after 150-minute absorption and 90-minute desorption cycles were 0.32 mol CO_2/mol amine for MEA, 0.93 mol CO_2/mol amine for TETA, 0.18 mol CO_2/mol amine for MDEA, and 0.63 mol CO_2/mol amine for the MDEA+TETA mixture. Notably, none of the absorbents achieved their maximum cyclic capacities under these operational parameters. This discrepancy arises from two primary constraints: 1) insufficient CO_2 saturation during the 150-minute absorption phase under low-flux, low-concentration, and low-partial-pressure CO_2 conditions, and 2) incomplete desorption within the 90-minute desorption period. These limitations demonstrate that the apparent cycling capacity inherently falls short of the theoretical maximum, thereby establishing the percentage ratio of apparent-to-maximum cycling capacity as a critical indicator for evaluating the practical performance gap between achievable and theoretical limits in cost-constrained CO_2 capture applications.

Further analysis of Fig. 6 reveals distinct performance patterns among the absorbents. MEA exhibited the highest apparent-to-maximum capacity ratio at 71.21%, primarily attributed to its rapid CO_2 absorption kinetics facilitated by primary amine reactivity [23]. TETA demonstrated a lower ratio of 66.27%, reflecting the molecular complexity of its multi-amine structure - the fixed 150-minute absorption duration proved insufficient for achieving full CO_2 loading across all available amino groups [24]. MDEA showed the poorest ratio at 41.46%, a consequence of its slow bicarbonate formation kinetics during absorption [25], requiring extended CO_2 exposure beyond 150 minutes for optimal loading. The MDEA+TETA blend achieved the most favorable balance with a 78.10% ratio, outperforming other formulations. This enhanced performance stems from synergistic interactions between the components: TETA contributes high absorption capacity through multiple reactive amino groups, while MDEA improves desorption efficiency via its bicarbonate formation pathway. The complementary mechanisms of tertiary amine (MDEA) and polyamine (TETA) components effectively optimize both absorption capacity and desorption kinetics, demonstrating the practical advantages of blended amine systems in cyclic CO_2 capture operations.

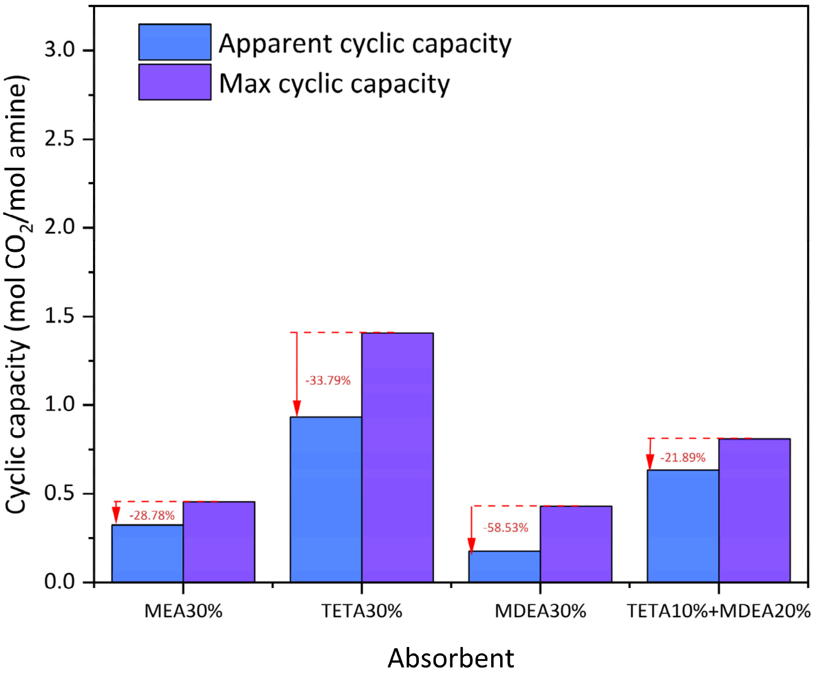

Fig 6. The apparent cyclic capacity and the ratio of apparent cyclic capacity to the maximum cyclic capacity of 30% MEA, 30% MDEA, 30% TETA and 20% MDEA+20% TETA witch absorbed CO_2 in 40 °C and PCO_2=15.15 Kpa for 150 min and desorbed in 125 °C for 90 min

3.3.2. 20 absorption-desorption Cycles Analysis

Fig. 7 illustrates the CO_2 loading variations and cyclic capacity evolution of four absorbents during 20 consecutive absorption-desorption cycles. Analysis of the rich solution loading and cyclic capacity reveals distinct degradation patterns: all absorbents except MDEA exhibited an initial increase followed by a gradual decrease in CO_2-rich solution loading throughout the cycles. The sky-blue trendline representing cyclic capacity demonstrates divergent stability profiles - MEA and TETA showed progressive capacity reduction with cycling (indicating poor stability), MDEA maintained near-constant capacity, while the MDEA+TETA blend displayed initial capacity enhancement followed by minor attenuation, suggesting superior cyclic stability.

As shown in Fig. 7(a), MEA's absorption loading increased cyclically until reaching a maximum of 0.549 mol CO_2/mol amine at the 13th cycle, slightly below its theoretical maximum capacity (0.556 mol CO_2/mol amine). Subsequent cycles exhibited progressive loading reduction, indicative of amine degradation under repeated cycling. This observation aligns with Jinkyu et al.'s findings [26], where MEA solution demonstrated similar degradation patterns after multiple cycles under saturation conditions. A degradation trendline constructed using MEA's maximum theoretical capacity and 20th-cycle loading reveals that post-12th cycle loadings consistently follow this degradation trajectory. Parallel analysis establishes a theoretical absorption trendline (assuming no degradation), predicting maximum capacity attainment at the 14th-15th cycle under ideal conditions. MEA's residual desorption loading (unreleased CO_2) progressively increased until stabilizing post-13th cycle. This phenomenon arises from two concurrent effects: 1) near-constant desorption capability throughout cycling [27], and 2) increasing absorption loading during initial cycles. The residual loading escalation reflects accumulated unreleased CO_2 proportional to absorbed quantities. Notably, MEA's cyclic capacity decreased from 0.34 mol CO_2/mol amine (1st cycle) to 0.31 mol CO_2/mol amine (20th cycle), demonstrating progressive loss of active amine groups available for cycling. This degradation mechanism explains why residual loading failed to decrease despite reduced absorption capacity after the 13th cycle, as compromised amine functionality simultaneously diminished both absorption capacity and desorption completeness.

Fig. 7(b) demonstrates that TETA exhibits absorption loading and residual desorption loading patterns similar to MEA during 20 absorption-desorption cycles. Notably, the 30% TETA solution maintained a nearly constant cyclic capacity of 0.94 mol CO_2/mol amine during the first five cycles. This stability arises from TETA's molecular structure containing multiple amino groups. Although amine degradation occurred during initial cycles, the short absorption/desorption durations prevented full participation of all amino groups in the process. The unreacted amino groups effectively compensated for active site loss caused by degradation, thereby maintaining maximum cyclic capacity. After the 5th cycle, when all amino groups had participated in the cycling process, TETA's capacity degradation pattern became analogous to MEA's behavior. This observation suggests that employing absorbents with excess reactive amino groups beyond single-cycle requirements can mitigate capacity degradation in multi-cycle CO_2 capture applications.

As shown in Fig. 7(c), MDEA displays minimal variation in absorption loading, residual desorption loading, and cyclic capacity throughout 20 cycles. The substantial gap between actual and maximum absorption loading stems from time-limited bicarbonate formation kinetics during absorption. Unlike carbamate-forming amines, MDEA's bicarbonate-based absorption mechanism avoids salt accumulation and exhibits exceptional chemical stability, resulting in negligible amine degradation during cycling. The complete desorption characteristics of bicarbonate compounds further ensure stable cyclic performance.

Fig. 7(d) reveals that the MDEA+TETA blend shares absorption loading characteristics with both MEA and TETA. However, its unique behavior manifests in stable residual desorption loading alongside increasing absorption loading during the first 12 cycles, driving cyclic capacity enhancement from 0.64 mol CO_2/mol amine (1st cycle) to 0.75 mol CO_2/mol amine (12th cycle). This phenomenon aligns with findings from Wei et al. [28] and He et al. [11], who identified that MDEA's tertiary amine groups catalyze the conversion of TETA-derived carbamates into bicarbonates. The catalytic effect modifies the absorption product distribution, reducing system enthalpy and enabling simultaneous absorption capacity enhancement and desorption completeness maintenance during initial cycling stages, which is shown in Eq. (11) and Eq. (12):

$$RNHCOO^- + H_2O \leftrightharpoons RNH_2 + HCO_3^- \tag{11}$$

$$R_2NCOO^- + H_2O \leftrightharpoons R_2NH + HCO_3^- \tag{12}$$

Therefore, the additional CO_2 absorbed through increased absorption loading is effectively converted into bicarbonate form due to the presence of tertiary amine groups, enabling facile desorption. During desorption, as bicarbonate concentration decreases, the tertiary amine facilitates continuous conversion of TETA carbamates into bicarbonates. This catalytic mechanism allows the blended solution to maintain high desorption efficiency within limited timeframes, preventing residual loading escalation despite increasing absorption capacity. Post-11th cycle, the MDEA+TETA blend exhibits gradual cyclic capacity reduction due to amine degradation. This demonstrates that hybrid absorbents combining polyamines (high capacity) with tertiary amines (carbamate-to-bicarbonate catalysis) can enhance cyclic performance in post-combustion CO_2 capture applications. The synergistic interaction enables sustained high cyclic absorption capacity over multiple operational cycles while maintaining system stability.

Based on this analysis, the cyclic capacity attenuation rate was calculated as the ratio between 1) the difference between maximum capacity and 20th-cycle capacity, and 2) the cycle interval between capacity peak and cycle termination. Higher attenuation rates indicate poorer cyclic stability. As shown in Table 1, the attenuation rates follow this descending order: TETA > MEA > MDEA+TETA > MDEA. This hierarchy aligns with experimental observations, confirming the cyclic stability ranking over 20 cycles as: MDEA > MDEA+TETA > MEA > TETA. The quantitative assessment validates that tertiary amine-based systems exhibit superior long-term stability compared to primary/polyamine counterparts in cyclic CO_2 capture operations.

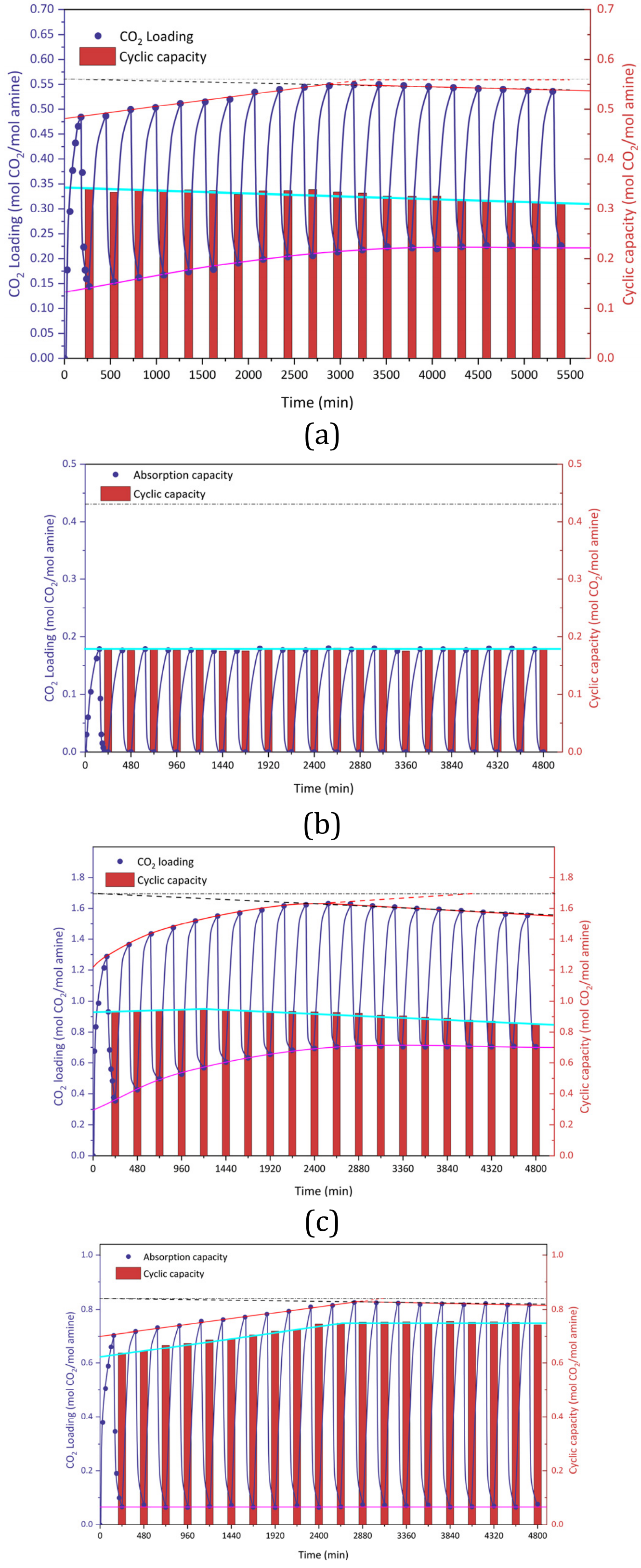

Fig 7. (a) Change of CO_2 load and circulating capacity in 20 cycles of 30% MEA solution, (B) Change of CO_2 Load and circulating capacity in 20 cycles of 30% TETA solution; (c) Change of CO_2 load and capacity in 20 cycles of 30% MDEA solution, (d) Change of CO_2 load and capacity in 20 cycles of 20% MDEA + 10% TETA solution

Table 1. Attenuation rate of circulating capacity of four absorbents

Absorbent	30% MEA	30% TETA	30% MDEA	20% MDEA+10% TETA
Cyclic capacity decay rate	0.00258503	0.00619914	0.00000585	0.00157669

4. Conclusion

(1) Under low-flux, low-partial-pressure CO_2 conditions, organic amine absorbents including MEA, TETA, MDEA, and MDEA-TETA blends demonstrate limited saturation absorption within constrained timeframes, coupled with incomplete desorption in most cases. The percentage ratio of apparent-to-maximum cyclic capacity effectively quantifies the performance gap between operational CO_2 capture efficiency and theoretical optimum under prioritized conditions. Furthermore, cyclic capacity evolution across 20 absorption-desorption cycles reveals stability variations among the four absorbents, primarily attributed to oxidative degradation and chemical decomposition during prolonged cycling.

(2) Absorbents with higher apparent-to-maximum cyclic capacity ratios exhibit smaller performance deviations from theoretical maxima during multi-cycle operations. The MDEA+TETA blend demonstrates this advantage through tertiary-polyamine synergy, achieving an apparent cyclic capacity of 0.81 mol CO_2/mol amine (78.1% of maximum capacity). This enhancement stems from MDEA's catalytic promotion of carbamate-to-bicarbonate conversion in TETA-derived absorption products, effectively bridging the gap between practical performance and theoretical potential.

(3) Cyclic stability ranking over 20 cycles follows: MDEA > MDEA+TETA > MEA > TETA. The MDEA+TETA hybrid uniquely combines TETA's multi-amine capacity with MDEA's catalytic bicarbonate conversion, demonstrating exceptional stability post-capacity optimization. After reaching 0.75 mol CO_2/mol amine at the 12th cycle, the blend maintained 0.74 mol CO_2/mol amine at the 20th cycle (1.33% attenuation). This performance validates that tertiary-polyamine hybridization enables stable cyclic absorption capabilities essential for long-term, multi-cycle CO_2 capture operations under low-concentration flue gas conditions. The synergistic mechanism effectively decouples absorption capacity from degradation susceptibility, addressing critical stability challenges in practical carbon capture applications.

References

[1] H. LEE J R: *Summary for Policymakers. In: Climate Change 2023: Synthesis Report*, (Geneva, Switzerland: IPCC), Vol. (2023),p.1-34.

[2] MYSIAK J, SURMINSKI S, THIEKEN A, et al.: Brief communication: Sendai framework for disaster risk reduction – success or warning sign for Paris? , Nat Hazards Earth Syst Sci, Vol. 16 (2016) No.10, p.2189-93.

[3] LIANG Dingcheng, YANG Lulu, XIE Xiang, et al.: Challenge of zeolite membranes in separating CO_2 from flue gas: Advances inresearch on binding forces between zeolite and carriers, Clean Coal Technology, Vol. 30 (2024) No.01, p.163-72.

[4] SHAW R, MUKHERJEE S: The development of carbon capture and storage (CCS) in India: A critical review, Carbon Capture Science & Technology, Vol. 2 (2022) p.100036.

[5] FIGUEROA J D, FOUT T, PLASYNSKI S, et al.: Advances in CO_2 capture technology—The U.S. Department of Energy's Carbon Sequestration Program, International Journal of Greenhouse Gas Control, Vol. 2 (2008) No.1, p.9-20.

[6] LIU H, QU J, BHATTI A H, et al.: A generic machine learning model for CO_2 equilibrium solubility into blended amine solutions, Separation and Purification Technology, Vol. 334 (2024) p.126100.

[7] YING Q, CHEN H, SHAO P, et al.: Core-shell magnetic ZIF-8@Fe3O4-carbonic anhydrase biocatalyst for promoting CO_2 absorption into MDEA solution, Journal of CO_2 Utilization, Vol. 49 (2021) p.101565.

[8] BAI L, ZHAO D, ZHONG X, et al.: Comprehensive technical analysis of CO_2 absorption into a promising blended amine of DEEA-HMDA, Chemical Engineering Science, Vol. 280 (2023) p.119025.

[9] FU H, XUE K, LI Z, et al.: Study on the performance of CO_2 capture from flue gas with ceramic and PTFE membrane contactors, Energy, Vol. 263 (2023) p.125677.

[10] AMIRKHANI F, DASHTI A, JOKAR M, et al.: Estimation of CO_2 solubility in aqueous solutions of commonly used blended amines: Application to optimised greenhouse gas capture, Journal of Cleaner Production, Vol. 430 (2023) p.139435.

[11] HE X, HE H, BARZAGLI F, et al.: Analysis of the energy consumption in solvent regeneration processes using binary amine blends for CO_2 capture, Energy, Vol. 270 (2023) p.126903.

[12] ZHANG R, LI Y, HE X, et al.: Investigation of the improvement of the CO_2 capture performance of aqueous amine sorbents by switching from dual-amine to trio-amine systems, Separation and Purification Technology, Vol. 316 (2023) p.123810.

[13] ZHANG R, LI T, ZHANG Y, et al.: CuO modified KIT-6 as a high-efficiency catalyst for energy-efficient amine solvent regeneration, Separation and Purification Technology, Vol. 300 (2022) p.121702.

[14] CHOI S Y, NAM S C, YOON Y I, et al.: Carbon Dioxide Absorption into Aqueous Blends of Methyldiethanolamine (MDEA) and Alkyl Amines Containing Multiple Amino Groups, Industrial & Engineering Chemistry Research, Vol. 53 (2014) No.37, p.14451-61.

[15] HAFIZI A, MOKARI M H, KHALIFEH R, et al.: Improving the CO_2 solubility in aqueous mixture of MDEA and different polyamine promoters: The effects of primary and secondary functional groups, Journal of Molecular Liquids, Vol. 297 (2020) p.111803.

[16] HU Yanlong, WANG Qiang, HU Dingkai, et al.: Selection of MDEA based phase change absorbers and carbondioxide capture performance, Clean Coal Technology, Vol. 30 (2024) No.06, p.158-70.

[17] WEN Zhen-zhen, HE Yue: CO_2 Capture Process Analysis for SMR Plant, Chemical Engineering Management, Vol. (2023) No.19, p.163-8.

[18] HAJI-SULAIMAN M Z, AROUA M K T: EQUILIBRIUM OF CO_2 IN AQUEOUS DIETHANOLAMINE(DEA) AND AMINO METHYL PROPANOL (AMP) SOLUTIONS, Chemical Engineering Communications, Vol. 140 (1995) p.157-71.

[19] LEE J I, OTTO F D, MATHER A E: Equilibrium between carbon dioxide and aqueous monoethanolamine solutions, Journal of Applied Chemistry and Biotechnology, Vol. 26 (1976) No.1, p.541-9.

[20] ARONU U E, GONDAL S, HESSEN E T, et al.: Solubility of CO_2 in 15, 30, 45 and 60 mass% MEA from 40 to 120°C and model representation using the extended UNIQUAC framework, Chemical Engineering Science, Vol. 66 (2011) No.24, p.6393-406.

[21] ALI B S, AROUA M K: Effect of Piperazine on CO 2 Loading in Aqueous Solutions of MDEA at Low Pressure, International Journal of Thermophysics, Vol. 25 (2004) No.6, p.1863-70.

[22] HUANG Yuhui: Research on degradation of blended amine solution for COz chemical absorption technology (Ph.D., Zhejiang University, 2021).

[23] KUMARI M, VEGA F, GALLEGO FERNáNDEZ L M, et al.: Liquid amine functional, aqueous blends and the CO_2 absorption capacity: Molecular structure, size, interaction parameter and mechanistic aspects, Journal of Molecular Liquids, Vol. 384 (2023) p.122288.

[24] ZHOU S, ZHU Y, XI H, et al.: Research on CO_2 capture performance and reaction mechanism using newly tetraethylenepentamine (TEPA) + monoethanolamine (MEA) mixed absorbent for onboard application, Chemical Engineering Journal, Vol. 485 (2024) p.149790.

[25] SHUNJI K, XIZHOU S, WENZE Y: Investigation of CO_2 desorption kinetics in MDEA and MDEA+DEA rich amine solutions with thermo-gravimetric analysis method, International Journal of Greenhouse Gas Control, Vol. 95 (2020) p.102947.

[26] IM J, HONG S Y, CHEON Y, et al.: Steric hindrance-induced zwitterionic carbonates from alkanolamines and CO_2: highly efficient CO_2 absorbents, Energy & Environmental Science, Vol. 4 (2011) No.10, p.4284-9.

[27] LIU H, NAMJOSHI O A, ROCHELLE G T: Oxidative Degradation of Amine Solvents for CO_2 Capture, Energy Procedia, Vol. 63 (2014) p.1546-57.

[28] WEI Wei, ZENG Lingzi, LIU Fengxia, et al.: Research on performance of mixed alcohol-amine in capturing low-concentration CO_2, Low-carbon Chemistry and Chemical Engineering, Vol. 48 (2023) No.03, p.116-22.